

# Carbon-based cores with polyglycerol shells – The importance of core flexibility for encapsulation of hydrophobic guests

Maike C. Lukowiak,<sup>a</sup> Benjamin Ziem,<sup>a</sup> Katharina Achazi,<sup>a</sup> Gesine Gunkel-Grabole,<sup>a</sup> Chris S. Popeney,<sup>a</sup> Bala N. S. Thota,<sup>a</sup> Christoph Böttcher,<sup>a</sup> Anke Krueger,<sup>b</sup> Zhibin Guan,<sup>c</sup> Rainer Haag<sup>\*,a</sup>

## Supporting Information

### Contents

<b>1. Experimental Section</b> .....	3
<b>Scheme S1.</b> Synthesis of <b>PE-PG</b> core-shell copolymer.....	4
<b>Scheme S2.</b> Synthesis of <b>ND-PG</b> core-shell nanoparticles.....	6
<b>2. References</b> .....	13
<b>3. Figures</b> .....	14
<b>Figure S1.</b> SEC-MALLS chromatogram of <b>PE-PG</b> .....	14
<b>Figure S2.</b> <sup>1</sup> H NMR of <b>PE-PG</b> core-shell copolymer.....	14
<b>Figure S3.</b> <sup>1</sup> H NMR of <b>ND-PG</b> core-shell nanoparticles.....	15
<b>Figure S4.</b> FTIR spectrum of oxidized nanodiamond <b>ND<sub>ox</sub></b> .....	15
<b>Figure S5.</b> FTIR spectrum of <b>ND-PG</b> core-shell nanoparticles.....	16
<b>Figure S6.</b> TGA profile of hydroxyl-functionalized polyethylene <b>PE-OH</b> .....	16
<b>Figure S7.</b> TGA profile of <b>PE-PG</b> core-shell copolymer.....	17
<b>Figure S8.</b> TGA profile of oxidized nanodiamond <b>ND<sub>ox</sub></b> .....	17
<b>Figure S9.</b> TGA profile of <b>ND-PG</b> core-shell nanoparticles.....	18

<b>Figure S10.</b> Pyrene UV spectra of <b>PE-PG</b> and <b>ND-PG</b> .....	18
<b>Figure S11.</b> Nile red UV spectra of <b>PE-PG</b> and <b>ND-PG</b> .....	19
<b>Figure S12.</b> DLS measurement result for <b>PE-PG</b> and <b>ND-PG</b> with NR.....	19
<b>Figure S13.</b> TEM image of oxidized nanodiamond <b>ND<sub>ox</sub></b> with staining.....	20
<b>Figure S14.</b> TEM image of <b>ND-PG</b> without staining.....	20
<b>Figure S15.</b> TEM images of <b>ND-PG</b> with staining.....	20
<b>Figure S16.</b> Cryo-TEM image of <b>PE-PG</b> core-shell copolymer.....	21
<b>Figure S17.</b> Cryo-TEM image of <b>ND-PG</b> core-shell nanoparticles.....	21
<b>Figure S18.</b> Confocal fluorescence microscopy image of A549 cells with <b>PE-PG</b> and NR (2 $\mu$ M)....	22
<b>Figure S19.</b> Confocal fluorescence microscopy image of A549 cells with <b>PE-PG</b> and NR (0.2 $\mu$ M).....	22
<b>Figure S20.</b> Confocal fluorescence microscopy image of A549 cells with <b>PE-PG</b> blank.....	23
<b>Figure S21.</b> Confocal fluorescence microscopy image of A549 cells with <b>ND-PG</b> and NR (0.2 $\mu$ M).....	23
<b>Figure S22.</b> Confocal fluorescence microscopy image of A549 cells with <b>ND-PG</b> blank.....	24
<b>Figure S23.</b> Confocal fluorescence microscopy image of A549 cells with NR blank.....	24
<b>Figure S24.</b> Confocal fluorescence microscopy image of A549 cells with NR (2 $\mu$ M).....	25
<b>Figure S25.</b> Confocal fluorescence microscopy image of A549 cells with NR (0.2 $\mu$ M).....	25
<b>Figure S26.</b> Confocal fluorescence microscopy image of A549 cells with medium.....	26
<b>Figure S27.</b> Confocal fluorescence microscopy image of A549 cells with PBS.....	26
<b>Table S1.</b> Flow cytometry data of A549 cells with <b>PE-PG</b> and <b>ND-PG</b> and controls.....	27

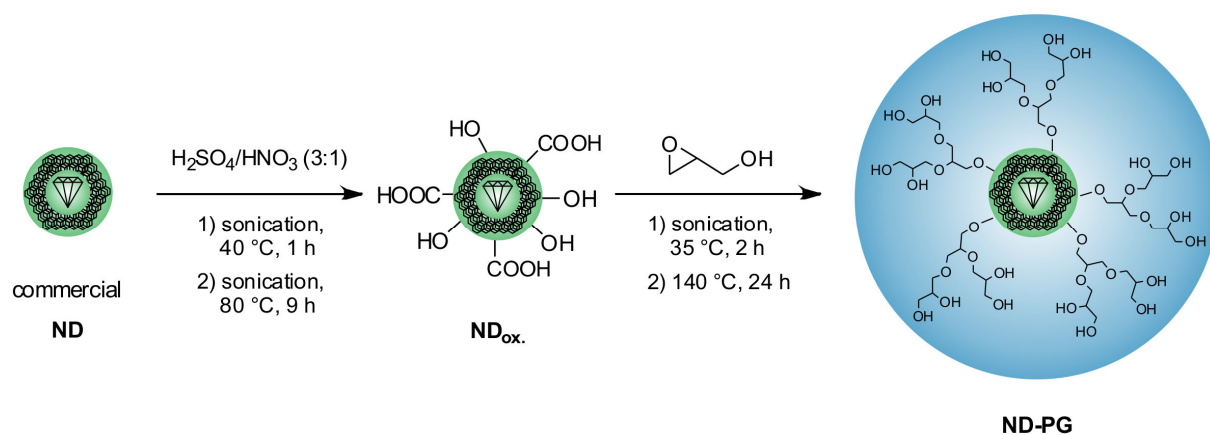
## 1. Experimental Section

**General Considerations.** All moisture and air-sensitive reactions were carried out in flame-dried glassware using magnetic stirring under a positive pressure of argon. Removal of organic solvents was accomplished by rotary evaporation and is referred to as concentrated in vacuo. All catalyst handling was carried out in a M.Braun glovebox filled with argon. NMR spectra were recorded on Jeol ECX 400, or Delta Jeol Eclipse 700 MHz spectrometer. NMRs were recorded in ppm and have been referenced to the indicated solvents. NMR data was reported as follows: chemical shift, multiplicity (s=singlet, d=doublet, t=triplet, q=quartet), integration, and coupling constant(s) in Hertz (Hz). Multiplets (m) were reported over the range (ppm) at which they appeared at the indicated field strength. Elemental analysis was measured on a Vario EL III elemental analyzer. IR spectra were measured on a Nicolet Avatar 320 FT-IR operating from 4000 - 400  $\text{cm}^{-1}$ . UV/Vis spectra were recorded on a Scinco S-3100 UV/Vis spectrometer. Fluorescence spectra were recorded on a Jasco FP-6500 fluorometer.

**Materials.** Anhydrous solvents were either purchased as extra dry from Acros or Aldrich and used as received or taken from a MBraun MB SPS-800 solvent purification system. Glycidol (Acros) was dried over  $\text{CaH}_2$ , distilled prior to use, and stored at 4 °C. Millipore quality water was obtained by purification of deionized water using a Millipore water purification system and had a minimum resistivity of 18.2  $\text{M}\Omega\cdot\text{cm}$ . Phosphate buffered saline (PBS; 10x concentrated; 90  $\text{g}\cdot\text{L}^{-1}$  NaCl, 7.95  $\text{g}\cdot\text{L}^{-1}$   $\text{Na}_2\text{HPO}_4$ , and 1.44  $\text{g}\cdot\text{L}^{-1}$   $\text{KH}_2\text{PO}_4$ ; pH 7.4) was purchased from Lonza (Köln, Germany) and was diluted to a 1x concentration (10 mM) by Milli-Q water prior to use. Unless otherwise stated, all other solvents and reagents were purchased from commercial suppliers and used as received. A mixture of 10 vol% ethylene (N45) in nitrogen (N50) was obtained from Air Liquide. Catalyst was stored in a glovebox under an argon atmosphere at -20 °C. The palladium  $\alpha$ -diimine catalyst,<sup>1-3</sup>  $\text{NaBAr}_4$  (Ar = 3,5-( $\text{CF}_3$ ) $_2\text{C}_6\text{H}_3$ ),<sup>4</sup> and TBDPS-protected comonomer<sup>5</sup> were synthesized according to the known literature procedures. Nanodiamond powder (grade “G-01”) was purchased from PlasmaChem GmbH.



was added dropwise over a period of 3.5 hours. After the final addition, the reaction was maintained at 120 °C for one hour and then cooled to room temperature and stirred overnight. The reaction was quenched with methanol (50 mL) and one gram of Dowex Monosphere 650C UPW ion-exchange resin and stirred for 3 hours. After filtration volatile solvents were removed in vacuo by rotary evaporation and diethyl ether was added to precipitate the polymer. The supernatant was discarded and the crude product was dissolved in distilled water. The turbid solution was centrifuged at 4000 rpm. The precipitate was discarded and the supernatant was purified by dialysis using regenerated cellulose membrane with 50,000 molecular weight cut-off in water and methanol to remove residual NMP and low MW polymers. The remaining crude product was purified by dialysis in water using cellulose ester membranes with a 300,000 molecular weight cut-off, changing the solvent three times every 12 hours. Finally, the remaining crude product was dialyzed in DMF using regenerated cellulose membranes with a 50,000 molecular weight cut-off, changing the solvent three times every 12 hours. The tube contents were collected and dried in vacuo, redissolved in distilled water, filtered through 0.45 regenerated cellulose (RC) syringe filter, and lyophilized to afford **PE-PG** as a highly viscous sticky white solid (2.07 g, 72%). <sup>1</sup>H NMR (400 MHz, CD<sub>3</sub>OD) δ 0.65 – 1.05 (m, broad, PE), 1.05 – 1.65 (m, broad, PE), 3.40 – 4.10 (m, broad, PG) ppm. To calculate of the degree of PG polymerization, the integration of resonances corresponding to PG in the <sup>1</sup>H NMR spectrum (Figure S1) were compared to the integration of the resonances corresponding to PE and yielded a molar ratio of 7.1/1 of glycerol to hydrocarbon (both olefin comonomers). An average value of 175 polymerized glycerol monomer units per hydroxyl group was calculated.



**Scheme S2.** Synthesis of **ND-PG** core-shell nanoparticles.

### Oxidation of Nanodiamond.

The oxidation of the nanodiamond (ND) was performed in a modified way based on the method reported in literature.<sup>7</sup> Nanodiamonds (0.50 g) were dispersed in a 3:1 mixture of conc. sulfuric acid (96 %, 24 mL) and nitric acid (65 %, 8 mL) in a 250 mL flask by using an ultrasonic bath for 1 h at 40 °C. Afterwards the dispersion was heated up to 80 °C under continuous usage of sonication for 9 h before cooling down to room temperature. The dispersion was diluted with distilled water and then centrifuged several times (each time 8850 g, 30 min) until a neutral pH was reached. The precipitates were collected and dialyzed for 3 d in distilled water before drying in the lyophilizer. A grey nanodiamond powder **ND<sub>ox</sub>** (415.7 mg) was obtained as product. EA: C: 79.32 %, H: 1.33 %, N: 2.62 %, O\*: 16.73 % (\*calculated based on the CHN values); bare ND before: C: 83.48 %, H: 1.42 %, N: 2.45 %, O\*: 12.65 %; FTIR:  $\nu_{\text{max}}/\text{cm}^{-1}$  3406br (OH), 1773w (C=O), 1636 (C=O), 1250w (C-O), 1105br (OH); bare ND before: 1716w (C=O), 1635w (C=O), 1267br (C-O), 1021w (OH).

### ND-PG Core-Shell Nanoparticle.

The preparation of the **ND-PG** was performed based on the method published by Komatsu et al.<sup>8,9</sup> The oxidized nanodiamonds **ND<sub>ox</sub>** (50.0 mg) and recently distilled glycidol (6.0 mL) were sonicated under argon atmosphere in an ultrasonic bath at 35 °C for 2 h to obtain a stable dispersion. After sonication the dispersion was continuously stirred at 140 °C for 24 h and then cooled down to room temperature before quenching with methanol (50.0 mL). The grayish dispersion was centrifuged five times (each

time 8850 g, 30 min) to remove unreacted glycidol and free polyglycerol. The precipitates were collected and dialyzed for 3 d in distilled water to remove remaining traces and methanol. **ND-PG** (423.7 mg, 85%) was obtained as a grayish solid after drying in the lyophilizer.  $^1\text{H NMR}$  (700 MHz,  $\text{CD}_3\text{OD}$ )  $\delta$  3.48 – 3.90 (m, broad, PG) ppm; EA: C: 50.06 %, H: 7.68 %, N: <0.01% O\*: 42.56 % (\*calculated based on the CHN values); FTIR:  $\nu_{\text{max}}/\text{cm}^{-1}$  3359br (OH) 2869s (CH), 1650vw (C=O), 1454w (CH), 1329w (CH), 1255w (C-O), 1067br (OH).

**Thermogravimetric analysis (TGA).** Thermogravimetric analysis was performed on a Linseis STA PT 1600 thermogravimetric analyzer using the Linseis Data Acquisition software with a temperature range from room temperature to 800 °C and a rate of 10 °C/min. Aluminium oxide crucibles (0.12 mL) were heated once to 800 °C before measuring the zero curve with empty crucible. Data was analyzed using Linseis Evaluation software.

**SEC-MALLS Characterization of Polymers.** Polyethylene copolymer **PE-OH** was characterized by size-exclusion chromatography (SEC) coupled to a multi-angle laser light scattering detector (MALLS) for obtaining the polymer MW ( $M_n$  and  $M_w$ ). Measurements were made on highly dilute fractions eluting from a SEC consisting of an Agilent 1100 solvent delivery system with isopump, manual injector, and an Agilent 1100 differential refractometer. A BI-MwA 7-angle light scattering detector from Brookhaven was coupled to the SEC to measure the MW for each fraction of the polymer eluted from the SEC columns. Three 30 cm columns were used (Polymer Laboratories PLgel Mixed C, 5  $\mu\text{m}$  particle size) to separate polymer samples. The mobile phase was THF and the flow rate was 1.0 mL/min. The columns were held at room temperature and the differential refractometer at 40 °C. A 100  $\mu\text{L}$  sample of a 10 mg/mL solution was injected. WinGPC Unity from PSS was used to acquire data from the 7 scattering angles (detectors) and the differential refractometer. The  $M_n$  and  $M_w$  data were obtained by following classical light scattering treatments.

**PE-OH:**  $M_n = 26$  kDa,  $M_w = 44$  kDa,  $M_w/M_n = 1.66$ .

The molecular weight distribution of the copolymer **PE-PG** was analyzed by SEC using the same solvent delivery system. Three 30 cm columns were used (PSS Suprema lux, 10  $\mu\text{m}$  particle size, hav-

ing 3000, 1000 and 100 Å pore sizes). The mobile phase was water with 0.1 M NaNO<sub>3</sub> and the flow rate was 1.0 mL/min. The columns were held at room temperature and the differential refractometer at 50 °C. A 100 µL sample of a 1 mg/mL solution was injected. WinGPC Unity from PSS was used to acquire data from the 7 scattering angles (detectors) and the differential refractometer. The  $M_n$  and  $M_w$  data were obtained by following classical light scattering treatments.

**PE-PG:**  $M_n = 268$  kDa,  $M_w = 960$  kDa,  $M_w/M_n = 3.59$ .

**Loading of the Nanocarriers.** Stock solutions of the stable **PE-PG** copolymer with a concentration of 10 mg/mL in PBS were prepared and diluted with PBS to 1 mg/mL prior to use. Solutions of **ND-PG** nanoparticles with the same concentrations were always freshly prepared before usage.

**General Procedure for the Encapsulation of Pyrene.** In a 5 mL glass vial 1 mg of pyrene (PY) was added followed by 3.0 mL of a stock solution of **PE-PG** or **ND-PG** (1 mg/mL) or PBS as control. The suspensions were stirred at 1200 rpm for 24 h, and the solutions were filtered through 0.45 µm regenerated cellulose (RC) syringe filters to remove unsolubilized PY. The clear solutions in water were then analyzed by various methods. The represented values are given as middle values with standard deviation of at least three measurements.

**General Procedure for the Encapsulation of Nile Red.**<sup>10</sup> A 5 mg/mL Nile red (NR) stock solution in tetrahydrofuran (THF) was prepared. 200 µL of the guest stock solution was transferred into 5 mL glass vials ( $\equiv$  1mg NR) and the solvent was evaporated. Afterwards, 3.0 mL of the **PE-PG** or **ND-PG** stock solutions (1 mg/mL) or PBS as control were added. The samples were stirred at 1200 rpm for 24 h. Subsequently, the NR samples were filtered through 0.45 µm RC syringe filters to remove unsolubilized NR. The clear solutions were then analyzed by various methods. The represented values are given as middle values with standard deviation of at least three measurements.

**UV/Vis Spectroscopy of Pyrene-PE-PG and ND-PG-Solutions.** All spectra were corrected by subtraction of the absorbance of **PE-PG** or **ND-PG** and the measured absorbance of the blank of the dye in PBS. For the transport capacity determination 1 mL of the aqueous solution of the different nanocar-

riers with solubilized PY was freeze-dried and redissolved in 2 mL methanol. The samples were filtered through 0.45  $\mu\text{m}$  RC syringe filters. The concentrations of PY in methanol were estimated using the molar extinction coefficient ( $\epsilon$ ) of 45,300  $\text{L}\cdot\text{mol}^{-1}\cdot\text{cm}^{-1}$  at 334  $\text{nm}$ <sup>11</sup> and applying Lambert-Beer law. Based on the  $M_n$  a loading of pyrene was determined to be 0.5 molecules of PY/PE-PG polymer, which is equal to  $0.40 \pm 0.06$  mg PY/g PE-PG carrier, which is equal to  $19.8 \times 10^{-7}$  mol PY/g PE-PG carrier. No significant uptake of pyrene could be found for ND-PG as carrier.

**UV/Vis Spectroscopy of Nile Red-PE-PG and ND-PG-Solutions.** All spectra were corrected by subtraction of the absorbance of PE-PG or ND-PG and the measured absorbance of the blank of the dye. For the transport capacity determination 1 mL of the aqueous solution of the different nanocarriers with solubilized NR was freeze-dried and redissolved in 2 mL methanol. The samples were filtered through 0.45  $\mu\text{m}$  RC syringe filters. The concentrations of NR in methanol were estimated using the molar extinction coefficient ( $\epsilon$ ) of 45,000  $\text{L}\cdot\text{mol}^{-1}\cdot\text{cm}^{-1}$  at 552  $\text{nm}$ <sup>12</sup> and applying Lambert-Beer law.

Based on the  $M_n$  a loading of Nile red was determined to be 0.5 molecules of NR/PE-PG polymer, which is equal to  $0.58 \pm 0.22$  mg NR/g PE-PG carrier, which is equal to  $18.2 \times 10^{-7}$  mol NR/g PE-PG carrier. For ND-PG the loading of Nile red was determined to be  $0.07 \pm 0.02$  mg NR/g ND-PG carrier, which is equal to  $2.2 \times 10^{-7}$  mol NR/g ND-PG carrier.

**Fluorescence Spectroscopy of Pyrene- PE-PG and ND-PG Solutions.** An excitation wavelength of 330 nm with an excitation bandwidth of 5 nm was used, with data collection every 1 nm at a rate of 100 nm/min, 1 s response time, and an emission bandwidth of 1 nm.

**Fluorescence Spectroscopy of Nile Red- PE-PG and ND-PG Solutions.** An excitation wavelength of 570 nm with an excitation bandwidth of 5 nm was used, with data collection every 1 nm at a rate of 100 nm/min, 1 s response time, and an emission bandwidth of 1 nm. The  $\lambda_{max}$  for Nile red emission in PBS in PE-PG was 633 nm.

**Dynamic Light Scattering Measurements.** Dynamic light scattering was performed on a Malvern Zetasizer Nano-ZS ZEN 3600 instrument equipped with a He-Ne laser (633 nm) and a fixed detector oriented at 173°. 1.0 mL of the solution to be analyzed was filtered through a 0.20 µm RC syringe filter into a 4.5 mL disposable cuvette (Roth) with a square aperture. The samples were allowed to equilibrate for at least 24 h before the measurement. The autocorrelation functions of backscattered light fluctuation were analyzed using Zetasizer DTS software from Malvern to determine the size distribution by intensity, volume, and number. The measurements were performed at 25 °C, equilibrating the system on this temperature for 120 s before. Samples were prepared in PBS at a concentration of 1 mg/mL.

**PE-PG:** Diameter  $119.1 \pm 2.5$  nm, 100 Int %, Ø PDI: 0.26.

**PE-PG** with encapsulated pyrene: Diameter  $120.2 \pm 2.6$  nm, 100 Int %, Ø PDI: 0.26.

**PE-PG** with encapsulated Nile red: Diameter  $146.0 \pm 4.3$  nm, 100 Int %, Ø PDI: 0.27.

**ND-PG:** Diameter  $159.3 \pm 5.2$  nm, 100 Int %, Ø PDI: 0.13.

**ND-PG** after encapsulation experiment with pyrene: Diameter  $154.4 \pm 4.3$  nm, 100 Int %, Ø PDI: 0.13.

**ND-PG** after encapsulation experiment with Nile red: Diameter  $160.1 \pm 4.1$  nm, 100 Int %, Ø PDI: 0.13.

### **Transmission Electron Microscopy (TEM).**

**Sample Preparation.** Every investigated compound was dissolved in Milli-Q water in a concentration of 1.0 mg/mL before adding a droplet (5 µL) of this solution on a pretreated carbon film covered with 200 mesh grids (Quantifoil Micro Tools GmbH, Jena, Germany). The supernatant of the droplet was removed with a standard filter paper to obtain ultra-thin compound layer on top of the carbon film. After this, the sample was directly stained with uranyl acetate (5 µL) and the supernatant was removed in the same way. All samples were dried at room temperature before transferring them to the transmission electron microscope. The pretreatment of the carbon film was done by 60 s of plasma coating using a BALTEC MED 020 (Leica Microsystems, Wetzlar, Germany) device.

**Measuring.** The dried samples were transferred into a Philips CM 12 transmission electron microscope (Philips Company, Amsterdam, Netherlands) using a standard sample holder. The investigations were performed according to the microscope low dose protocol at a calibrated primary magnification of 58,300x and an accelerating voltage of 100 kV (LaB6-illumination). All images were recorded on Kodak SO-136 electron image film with a defocus of -300 nm.

**Observations.** The oxidized nanodiamonds  $\text{ND}_{\text{ox}}$  with the size average of around 5 nm as well as the PG functionalized nanodiamonds **ND-PG** show an aggregation behavior. In case of the functionalized nanodiamonds **ND-PG**, the aggregates had a non-spherical geometry and the size varied between 50 - 200 nm. The size of the aggregates for  $\text{ND}_{\text{ox}}$  were even larger. However, the significant difference between the samples is the detectable core-shell architecture of the functionalized particles.

#### **Cryogenic Transmission Electron Microscopy (cryo-TEM).**

**Sample Preparation.** For all preparations aqueous polymer solutions at a concentration of 1 mg/mL were used. Droplets of the sample solution (5  $\mu\text{L}$ ) were applied to perforated (1  $\mu\text{m}$  hole diameter) carbon film covered 200 mesh grids (R1/4batch of Quantifoil Micro Tools GmbH, Jena, Germany), which had been hydrophilized prior to use by a 60 s plasma treatment at 8 W in a BALTEC MED 020 (Leica Microsystems, Wetzlar, Germany) device. The supernatant fluid was removed with a filter paper until an ultra-thin layer (100 – 200 nm) was obtained spanning the holes of the carbon film. The samples were immediately vitrified by propelling the grids into liquid ethane at its freezing point (90 K) operating a guillotine-like plunging device.

**Cryo-TEM.** The vitrified samples were transferred under liquid nitrogen into a Tecnai F20 FEG transmission electron microscope (FEI Company, Oregon, USA) using the Gatan (Gatan Inc., California, USA) cryoholder and -stage (Model 626). Microscopy was carried out at 94 K sample temperature using the microscopes low dose protocol at a calibrated primary magnification of 50,000 $\times$  and an accelerating voltage of 160 kV (FEG-illumination). Images were recorded using an EAGLE 2k-CCD device (FEI Company, Oregon, USA) at 2048 by 2048 pixel size. The defocus was chosen in all cases to be 5 $\mu\text{m}$ .

## **Biological Studies.**

**Cell Culture.** The epithelial human lung cancer cell line A549 (adenocarcinomic human alveolar basal epithelial cell line) was routinely propagated in DMEM medium supplemented with 10 % fetal calf serum (FCS), 2 % glutamine, and 100 U/mL penicillin/streptomycin (all media and supplements were ordered from Gibco). Cells were cultured at 37 °C with 5 % CO<sub>2</sub> and split 1:5 to 1:10 when they were 90 % confluent (two to three times a week).

**Confocal Laser Scanning Microscopy (cLSM).** For cLSM 50,000 A549 cells were seeded on 9 mm glass coverslips in each well of a 24-well plate and cultured for 24 h before adding the Nile red loaded nanocarriers or the unloaded nanocarriers, only media, or PBS as control. For the **PE-PG** nanocarrier we used a concentration series. Samples were diluted in cell culture medium. After 4 hours incubation, cells were washed 3 times with PBS and fixed with 4 % paraformaldehyde (PFA) for 20 min at room temperature. Afterwards, cell nuclei were stained with 4',6-diamidino-2-phenylindole (DAPI). Cells were observed and imaged using a confocal laser scanning microscope (Leica DMI6000CSB stand) and the Leica LAS AF software.

**Flow Cytometry.** For flow cytometry 150,000 A549 cells were seeded in each well of a 24-well plate and cultured for 24 h before adding the Nile red loaded nanocarriers or the controls. After 4 hours of incubation, cells were washed 3 times with PBS and detached by trypsin. The detached cells were transferred to a flow cytometry tube and centrifuged at 138 x g for 5 min. Supernatants were discarded and cells were fixed with 4 % cold PFA for 10 min at 4 °C. To remove the PFA cells were centrifuged at 138 x g for 5 min. Supernatants were discarded and cells were resuspended in PBS supplemented with 1 % FCS and 0.1 % sodium azide. Fluorescence intensity of the cells was measured in a FACScantor (Becton Dickinson, Heidelberg, Germany). Three times 10,000 events were detected per sample and the median fluorescence intensity for each measurement was determined using Flowing Software 2.0.

## 2. References

1. E. V. Salo and Z. Guan, *Organometallics*, 2003, **22**, 5033–5046.
2. S. Mecking, L. K. Johnson, L. Wang, and M. Brookhart, *J. Am. Chem. Soc.*, 1998, **120**, 888–899.
3. L. K. Johnson, C. M. Killian, and M. Brookhart, *J. Am. Chem. Soc.*, 1995, **117**, 6414–6415.
4. N. A. Yakelis and R. G. Bergman, *Organometallics*, 2005, **24**, 3579–3581.
5. G. Chen, X. S. Ma, and Z. Guan, *J. Am. Chem. Soc.*, 2003, **125**, 6697–6704.
6. C. S. Popeney, M. C. Lukowiak, C. Böttcher, B. Schade, P. Welker, D. Mangoldt, G. Gunkel, Z. Guan, and R. Haag, *ACS Macro Lett.*, 2012, **1**, 564–567.
7. V. F. Loktev, V. I. Makal'skii, I. V. Stoyanova, A. V. Kalinkin, and V. A. Likholobov, *Carbon*, 1991, **29**, 817–819.
8. L. Zhao, T. Takimoto, M. Ito, N. Kitagawa, T. Kimura, and N. Komatsu, *Angew. Chem. Int. Ed.*, 2011, **50**, 1388–1392.
9. L. Zhao, T. Chano, S. Morikawa, Y. Saito, A. Shiino, S. Shimizu, T. Maeda, T. Irie, S. Aonuma, H. Okabe, T. Kimura, T. Inubushi, and N. Komatsu, *Adv. Funct. Mater.*, 2012, **22**, 5107–5117.
10. E. Fleige, K. Achazi, K. Schaletzki, T. Triemer, and R. Haag, *J. Control. Release*, 2014, **185**, 99–108.
11. J. J. Kiefer, P. Somasundaran, and K. P. Ananthapadmanabhan, in *Polymer Solutions, Blends, and Interfaces*, eds. I. Noda and D. N. Rubingh, Elsevier Science Publishers B.V., 1992, p. 430.
12. R. P. Haugland, in *Handbook of Fluorescent Probes and Research Chemicals*, Molecular Probes Inc., Eugene, OR, USA, sixth ed., 1996.

### 3. Figures

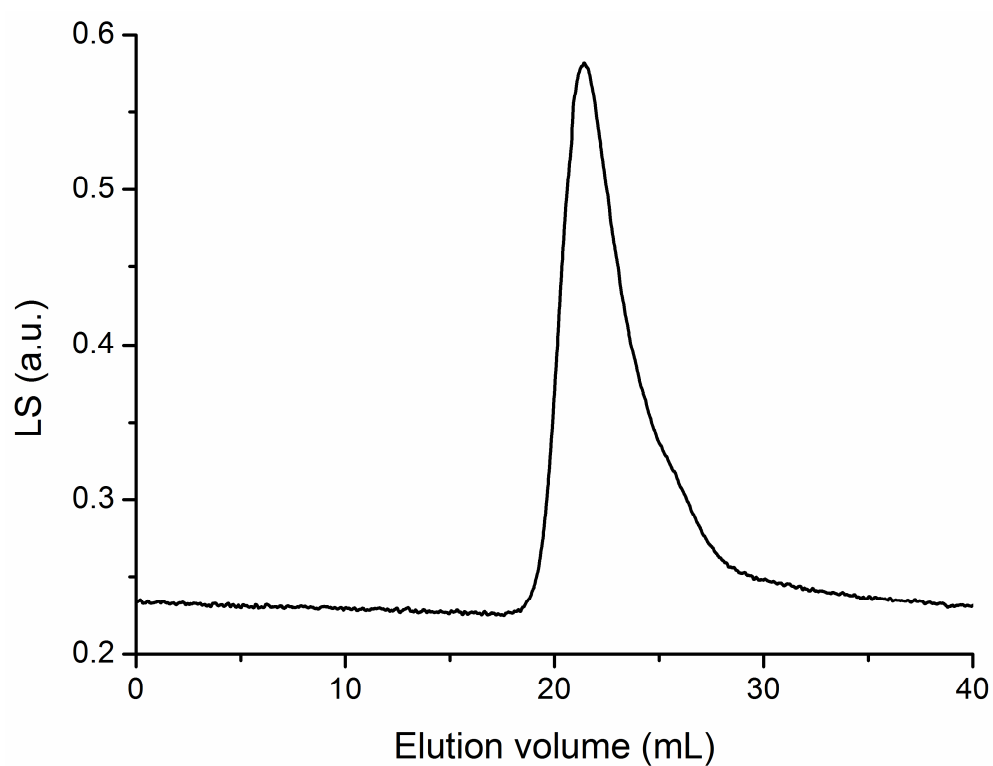


**Figure S1.** SEC-MALLS chromatogram of **PE-PG** using water with 0.1 M NaNO<sub>3</sub> as the eluent showing the light scattering (LS) signal from the 105° angle.

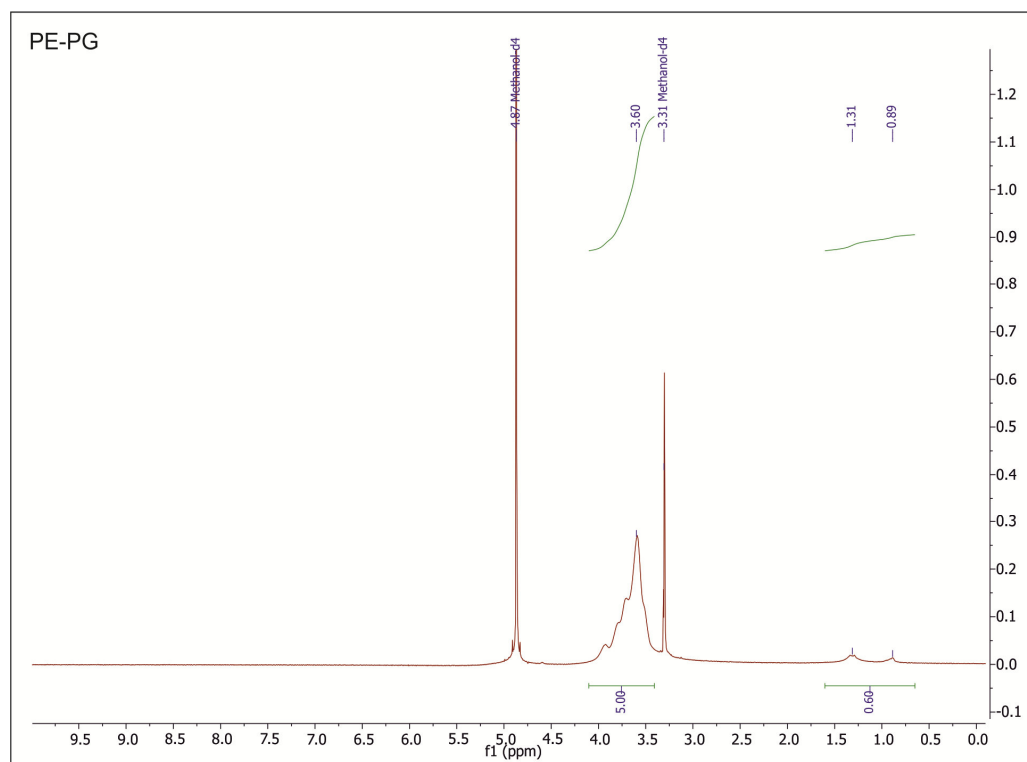


**Figure S2.** <sup>1</sup>H NMR (400 MHz, CD<sub>3</sub>OD) of **PE-PG** core-shell copolymer.

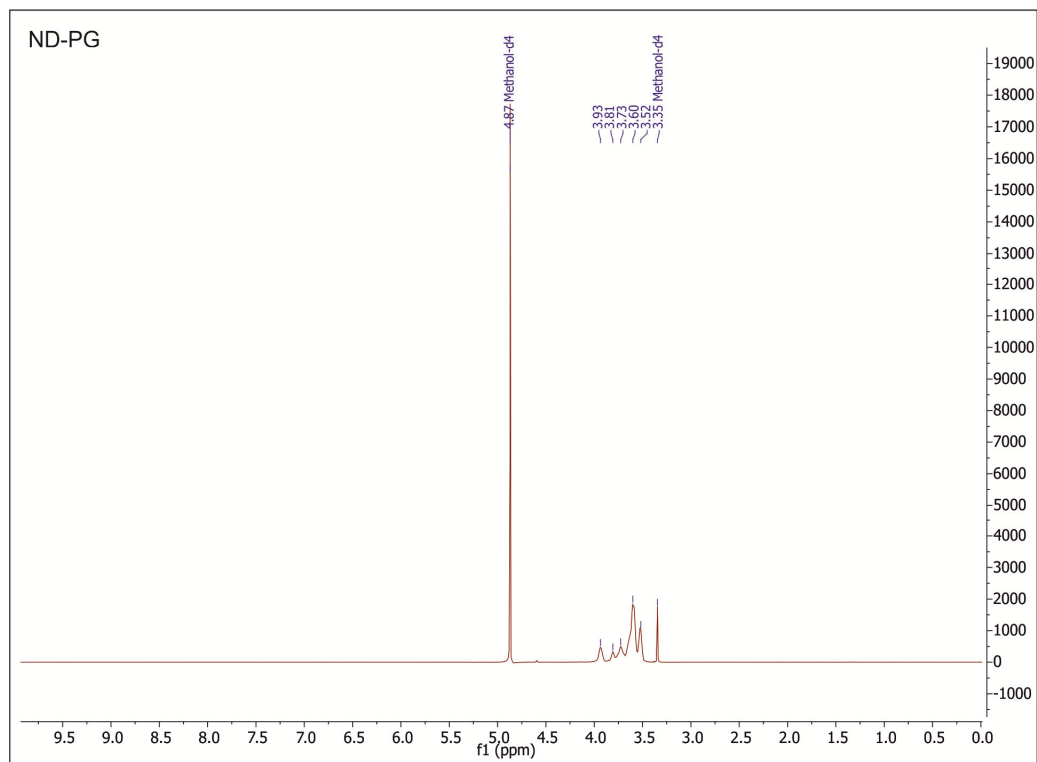


**Figure S3.**  $^1\text{H}$  NMR (700 MHz,  $\text{CD}_3\text{OD}$ ) of **ND-PG** core-shell nanoparticles.

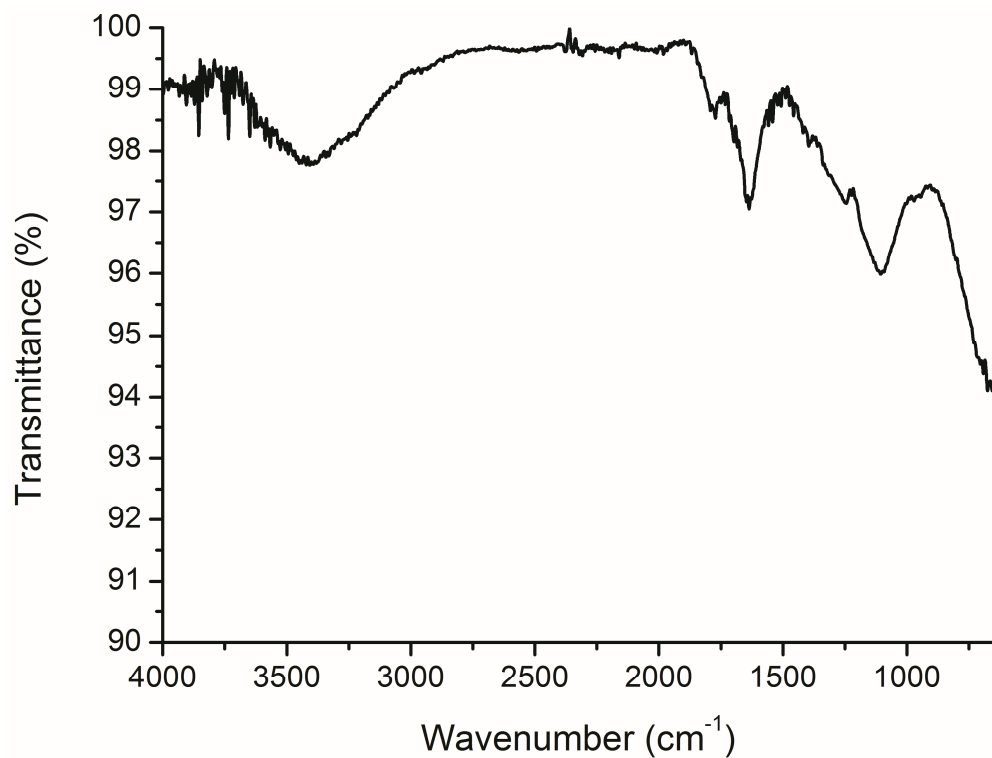


**Figure S4.** FTIR spectrum of oxidized nanodiamond  $\text{ND}_{\text{ox}}$ .

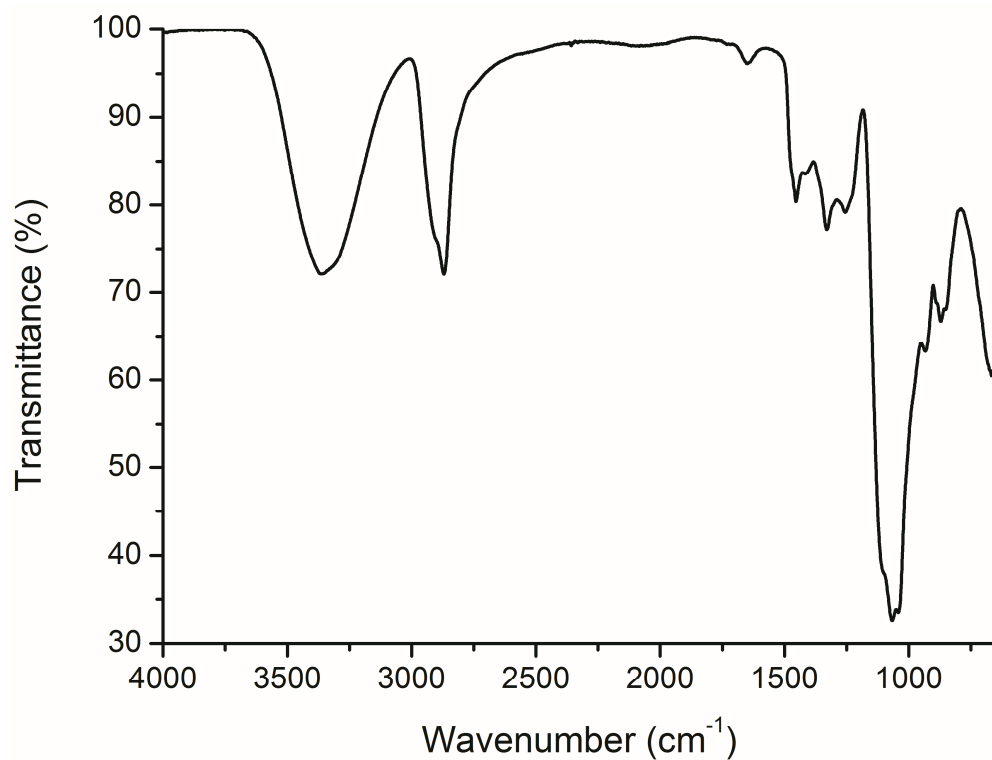


**Figure S5.** FTIR spectrum of **ND-PG** core-shell nanoparticles.

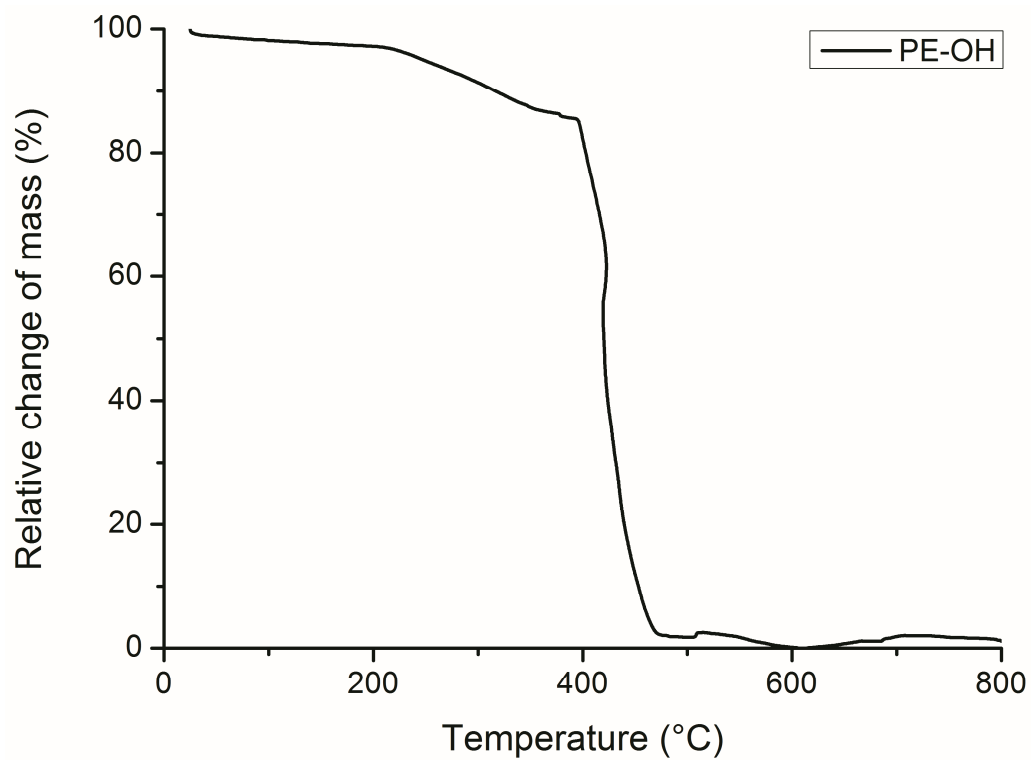


**Figure S6.** Normalized TGA profile of hydroxyl functionalized polyethylene **PE-OH**.

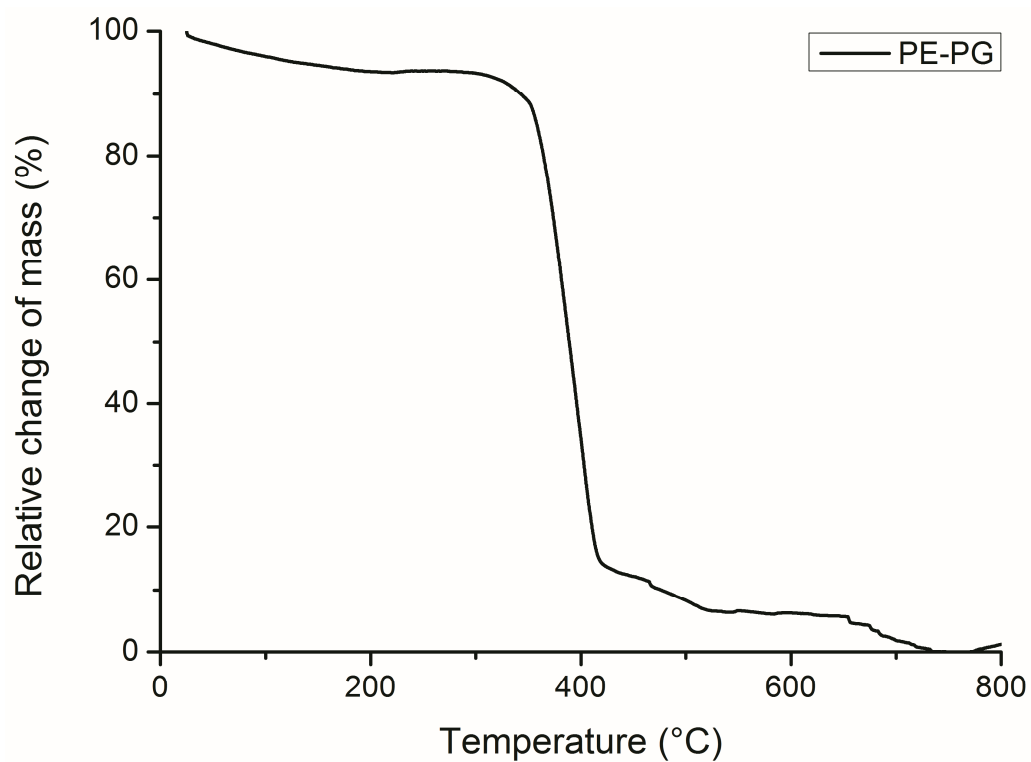


**Figure S7.** Normalized TGA profile of **PE-PG** core-shell copolymer.

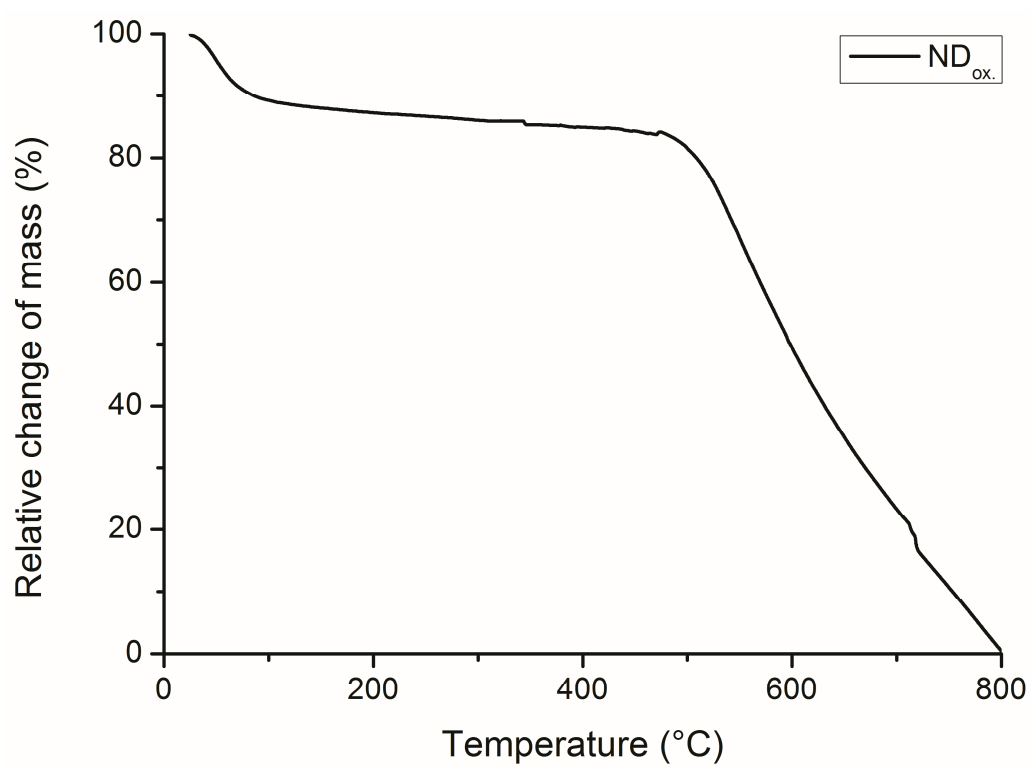


**Figure S8.** Normalized TGA profile of oxidized nanodiamond **ND<sub>ox</sub>**.

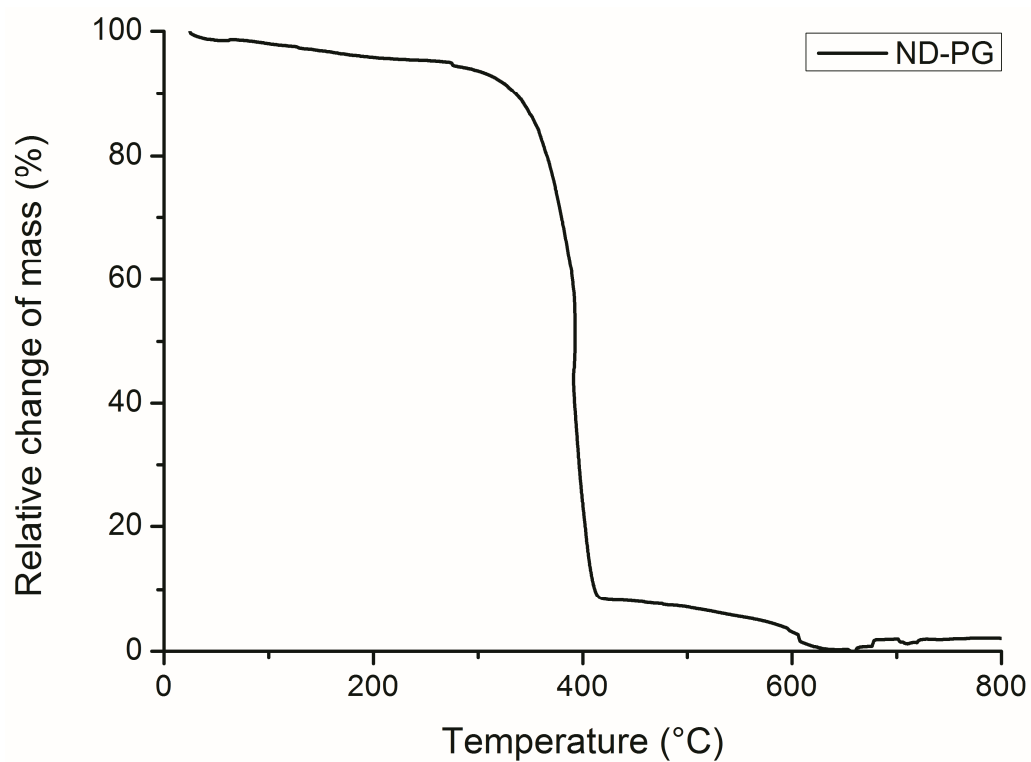


**Figure S9.** Normalized TGA profile of **ND-PG** core-shell nanoparticles.

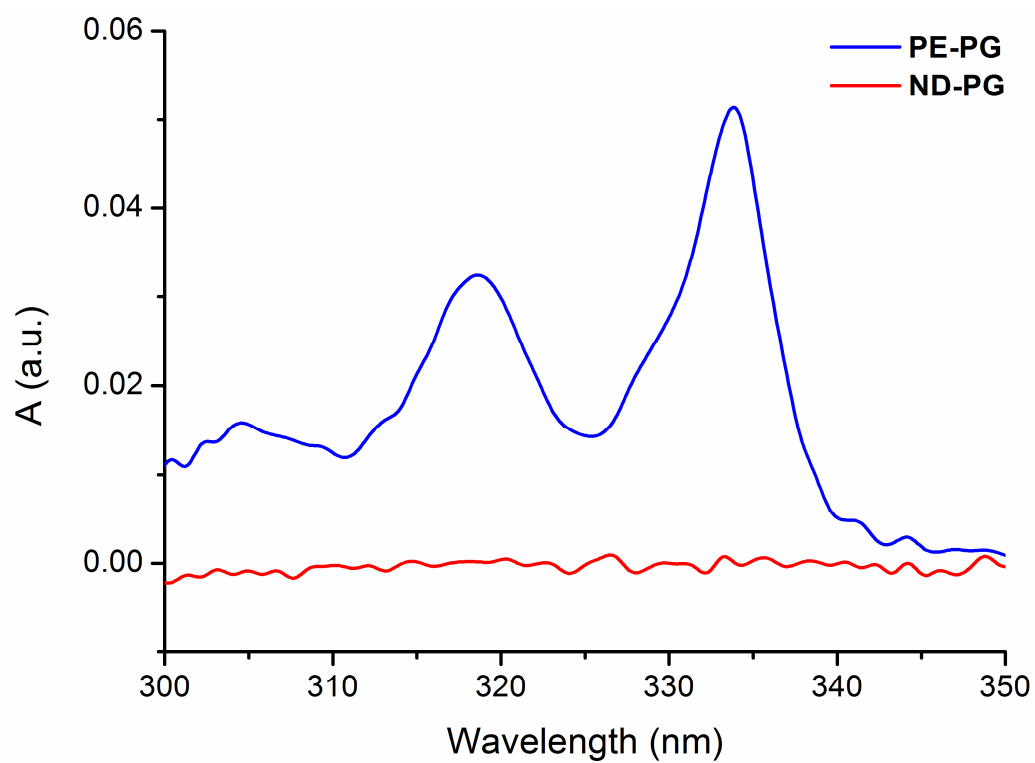


**Figure S10.** Pyrene UV spectra of **PE-PG** (blue) and **ND-PG** (red) both measured at concentrations of 1.0 mg/mL in MeOH after lyophilization of the original PBS solution from the encapsulation experiment.

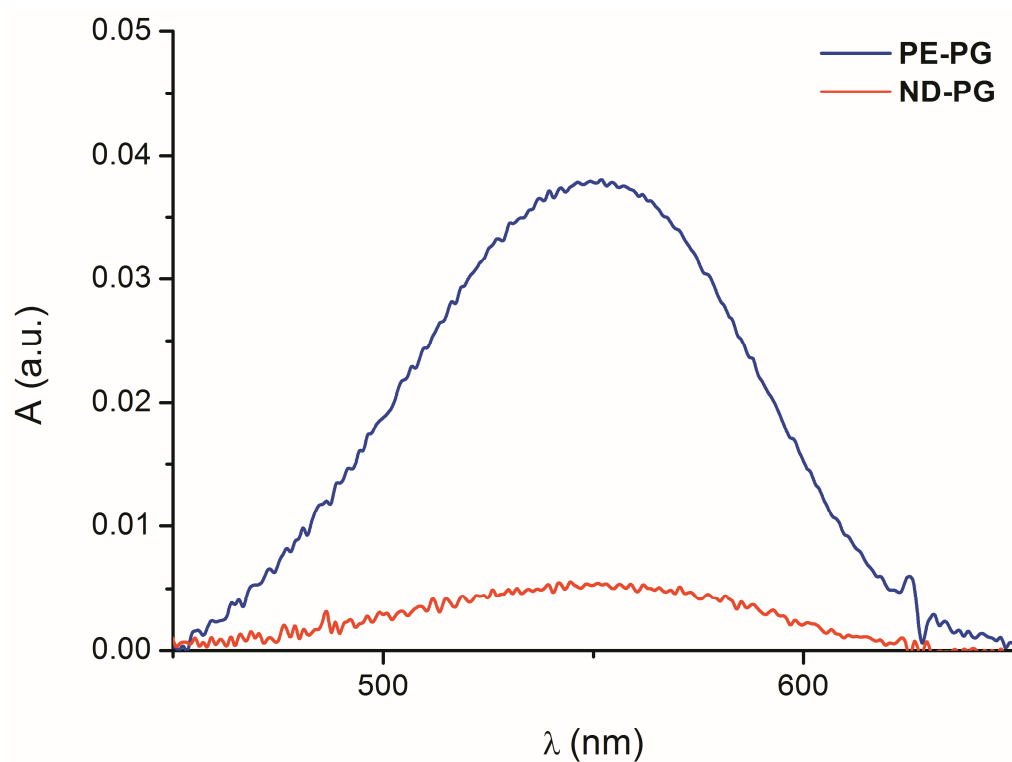


**Figure S11.** Nile red UV spectra of **PE-PG** (blue) and **ND-PG** (red) both measured at concentrations of 1.0 mg/mL in MeOH after lyophilization of the original PBS solution from the encapsulation experiment.

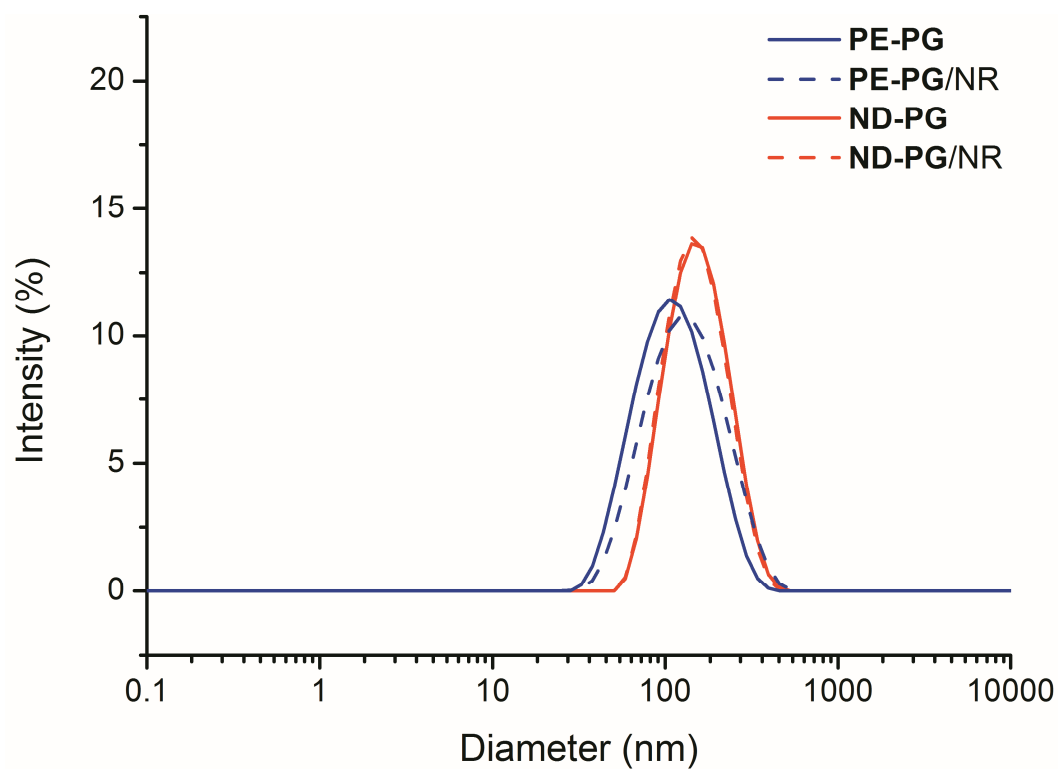


**Figure S12.** DLS measurement result for the intensity distribution of unloaded **PE-PG** (blue, continuous line) and **ND-PG** (red, continuous line) and after encapsulation experiment with NR (each with dashed line) in PBS.

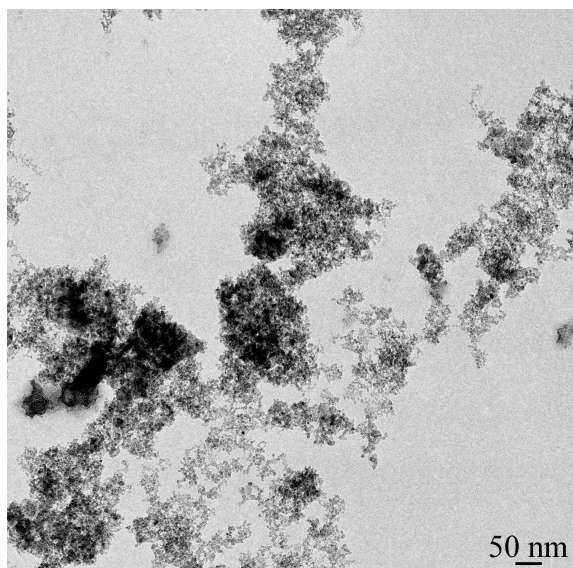


**Figure S13.** TEM image of oxidized nanodiamond ND<sub>ox</sub> using uranyl acetate staining.

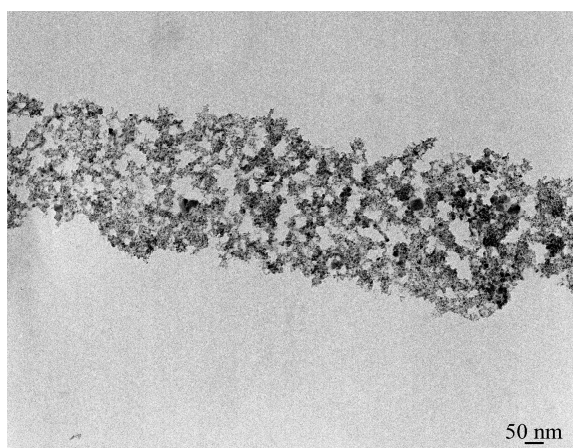


**Figure S14.** TEM image of ND-PG core-shell nanoparticles without staining.

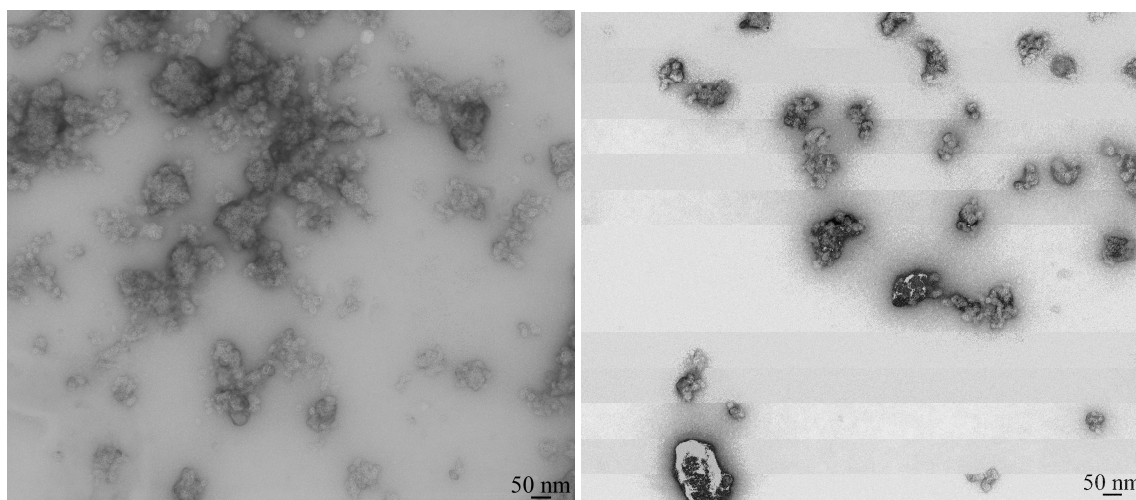


**Figure S15.** Two TEM images of ND-PG core-shell nanoparticles using uranyl acetate staining.

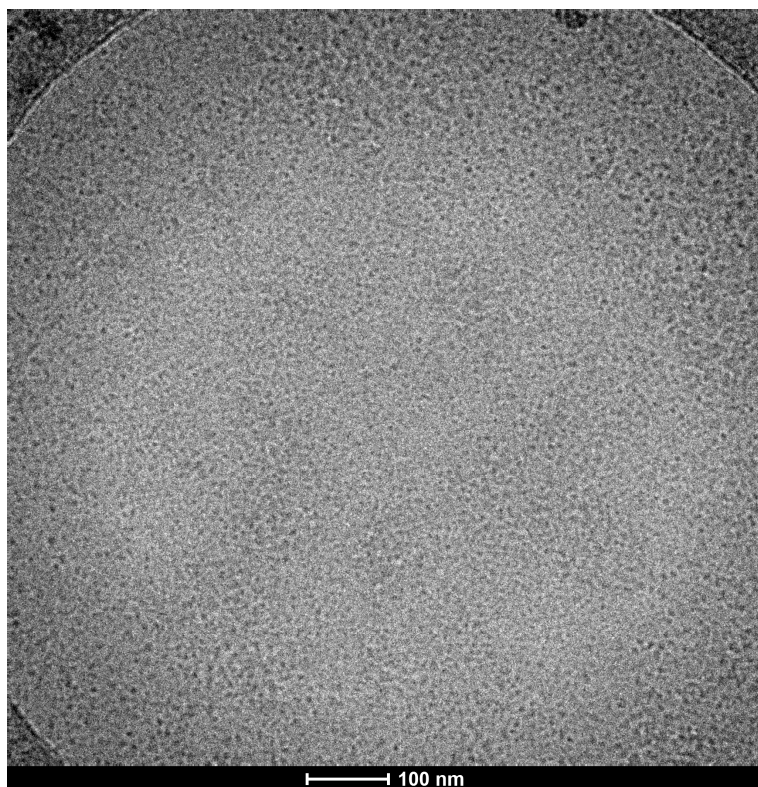


**Figure S16.** Cryo-TEM image of **PE-PG** core-shell copolymer.

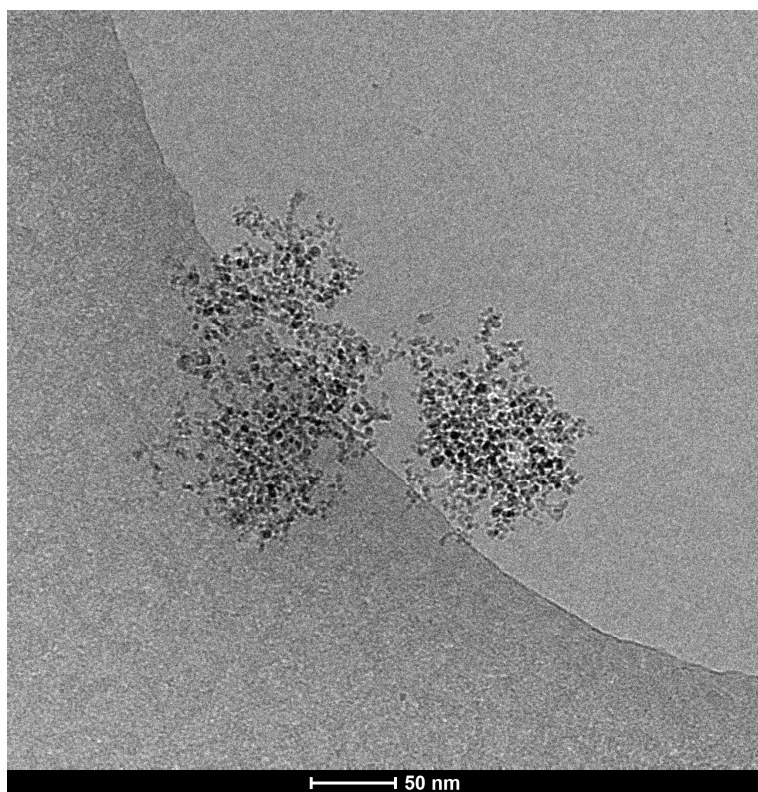


**Figure S17.** Cryo-TEM image of **ND-PG** core-shell nanoparticles.

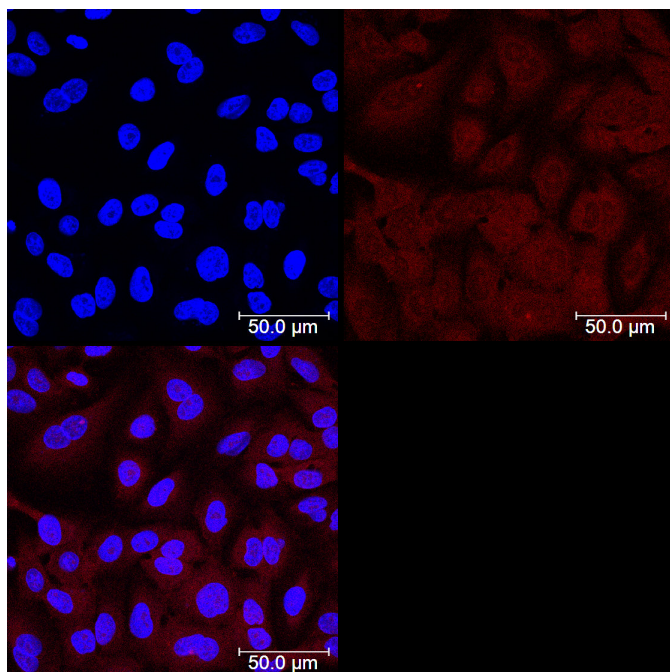


**Figure S18.** Confocal fluorescence microscopy image of A549 cells incubated for 4 h with **PE-PG** of a concentration of 1 mg/mL with NR (red,  $c = 2 \mu\text{M}$ ). Cell nuclei were stained with DAPI (blue). Top left: blue channel, top right: red channel, bottom left: merged red and blue channel.

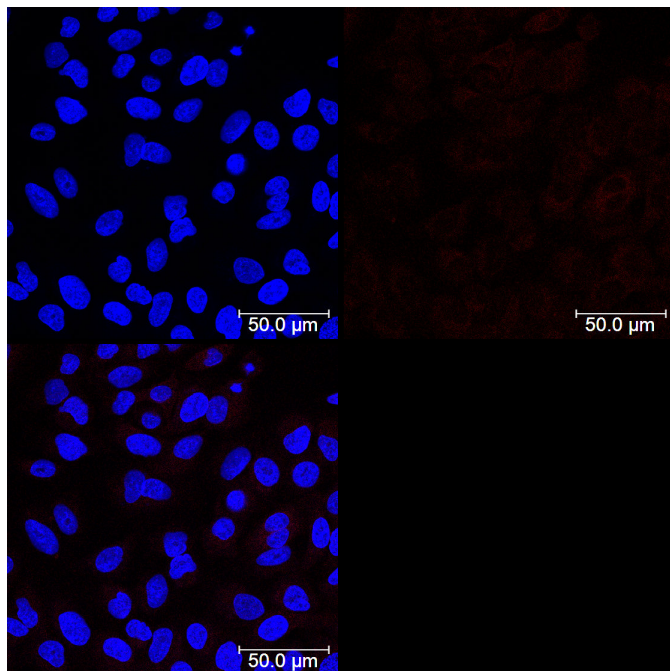


**Figure S19.** Confocal fluorescence microscopy image of A549 cells incubated for 4 h with **PE-PG** of a concentration of 0.1 mg/mL with NR (red,  $c = 0.2 \mu\text{M}$ ). Cell nuclei were stained with DAPI (blue). Top left: blue channel, top right: red channel, bottom left: merged red and blue channel.

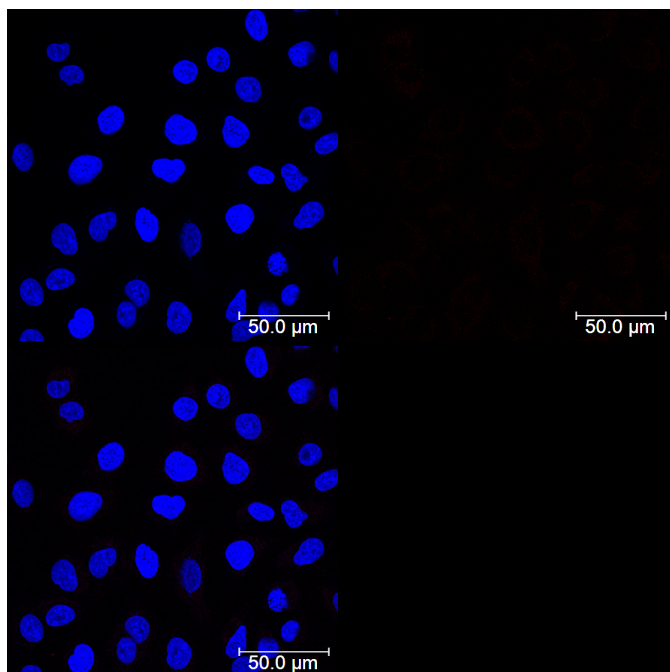


**Figure S20.** Confocal fluorescence microscopy image of A549 cells incubated for 4 h with **PE-PG** of a concentration of 1 mg/mL without NR as control. Cell nuclei were stained with DAPI (blue). Top left: blue channel, top right: red channel, bottom left: merged red and blue channel.

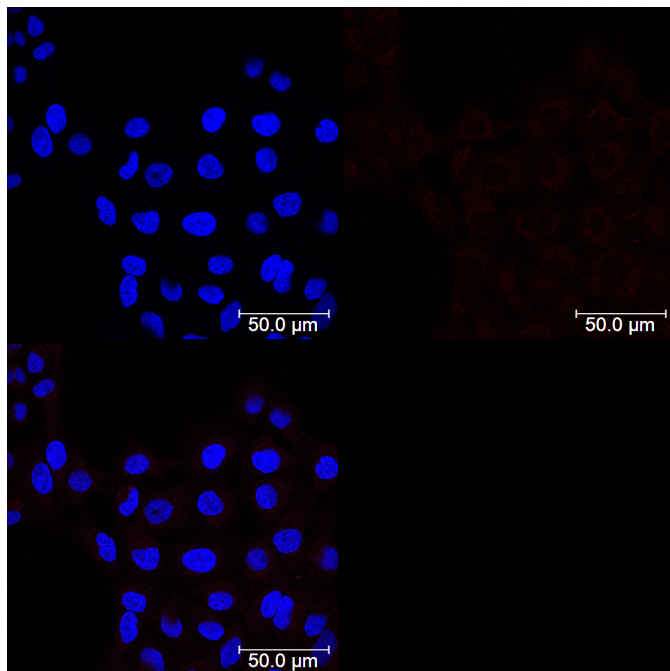


**Figure S21.** Confocal fluorescence microscopy image of A549 cells incubated for 4 h with **ND-PG** of a concentration of 1 mg/mL with NR (red,  $c = 0.2 \mu\text{M}$ ). Cell nuclei were stained with DAPI (blue). Top left: blue channel, top right: red channel, bottom left: merged red and blue channel.

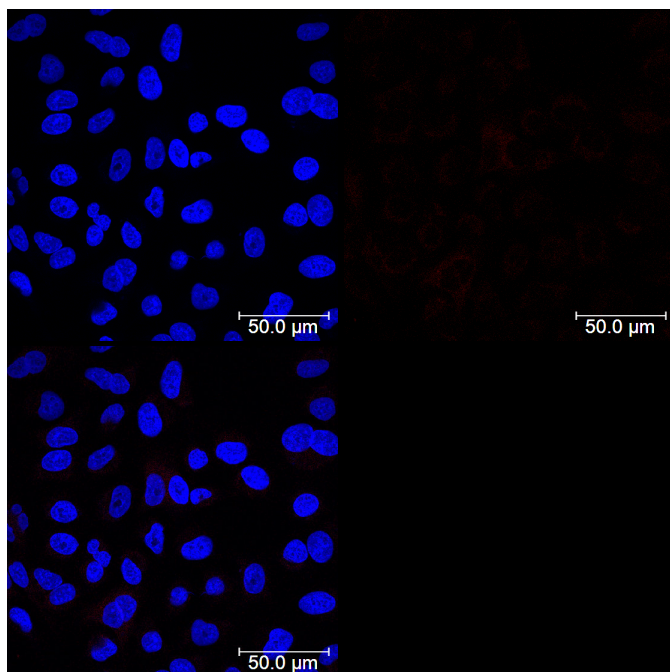


**Figure S22.** Confocal fluorescence microscopy image of A549 cells incubated for 4 h with **ND-PG** of a concentration of 1 mg/mL without NR as control. Cell nuclei were stained with DAPI (blue). Top left: blue channel, top right: red channel, bottom left: merged red and blue channel.

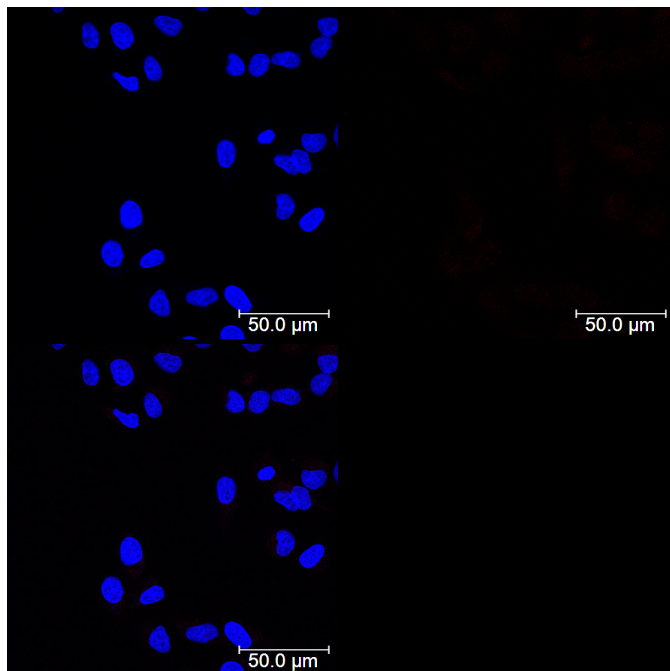


**Figure S23.** Confocal fluorescence microscopy image of A549 cells incubated for 4 h with the solution of the blank experiment of NR (red) without presence of any carrier as control. Cell nuclei were stained with DAPI (blue). Top left: blue channel, top right: red channel, bottom left: merged red and blue channel.

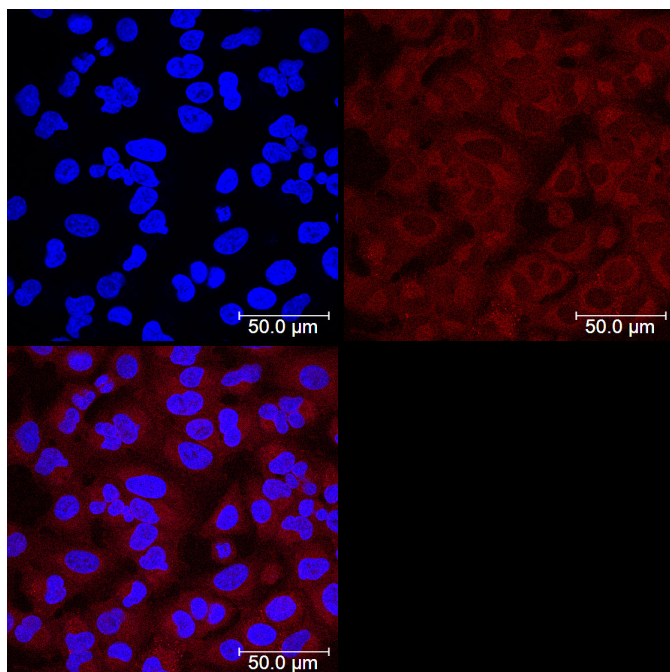


**Figure S24.** Confocal fluorescence microscopy image of A549 cells incubated for 4 h with NR (red) of a concentration of 2  $\mu\text{M}$  as positive control. Nile Red was initially dissolved in DMSO and diluted to the required concentration by medium. Cell nuclei were stained with DAPI (blue). Top left: blue channel, top right: red channel, bottom left: merged red and blue channel.

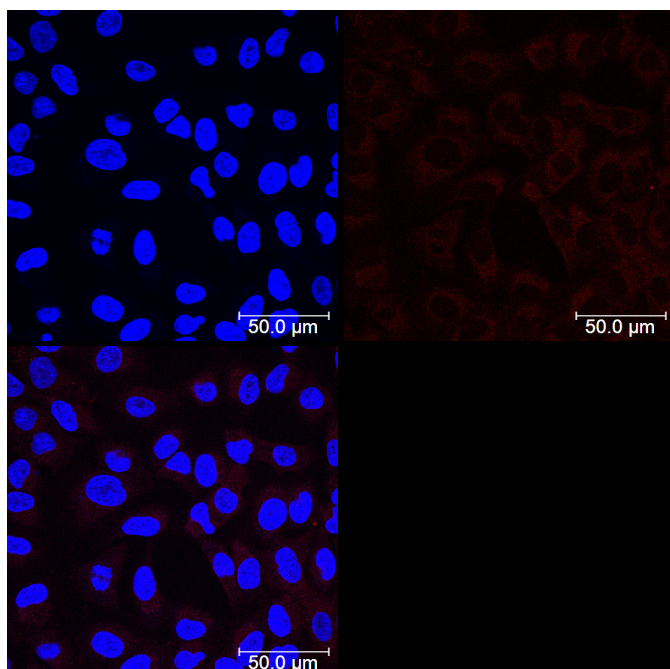


**Figure S25.** Confocal fluorescence microscopy image of A549 cells incubated for 4 h with NR (red) of a concentration of 0.2  $\mu\text{M}$  as positive control. Nile Red was initially dissolved in DMSO and diluted to the required concentration by medium. Cell nuclei were stained with DAPI (blue). Top left: blue channel, top right: red channel, bottom left: merged red and blue channel.

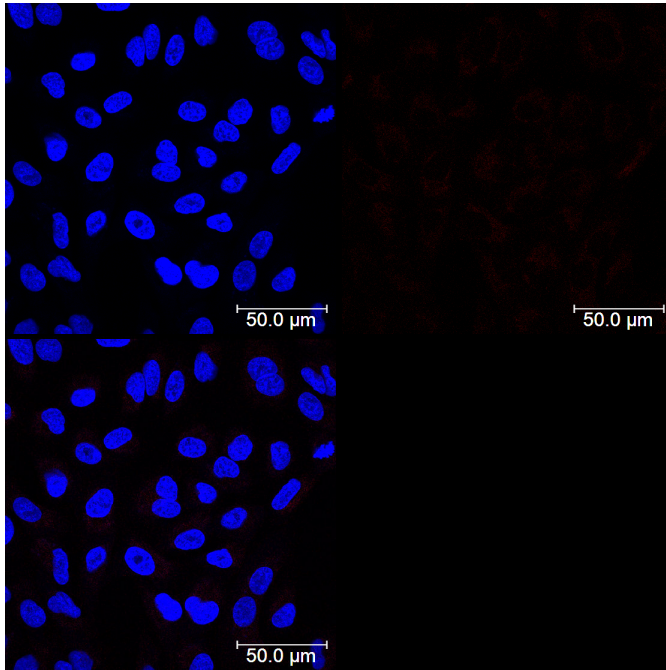


**Figure S26.** Confocal fluorescence microscopy image of A549 cells incubated for 4 h with medium as negative control. Cell nuclei were stained with DAPI (blue). Top left: blue channel, top right: red channel, bottom left: merged red and blue channel.

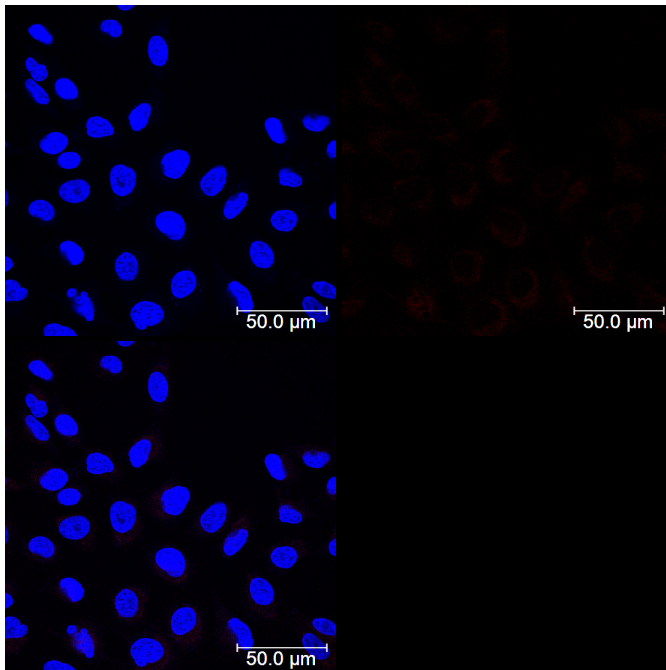


**Figure S27.** Confocal fluorescence microscopy image of A549 cells incubated for 4 h with PBS as negative control. Cell nuclei were stained with DAPI (blue). Top left: blue channel, top right: red channel, bottom left: merged red and blue channel.

**Table S1.** Data from the flow cytometry measurements of the cell uptake of **PE-PG/NR** and **ND-PG/NR** for A549 cell line with 4 hours incubation.

<i>Sample</i>	<i>c<sub>nanocarrier</sub> (mg/mL)</i>	<i>c<sub>NR</sub> (μM)</i>	<i>Median fluorescence intensity (a.u.)</i>		
<b>PE-PG</b>	1	2	3715.47	3707.13	3714.08
<b>PE-PG</b>	0.5	1	3135.84	2935.68	2863.40
<b>PE-PG</b>	0.2	0.4	1102.27	1141.19	1120.34
<b>PE-PG</b>	0.1	0.2	492.06	501.79	518.47
<b>PE-PG</b>	1	0	16.68	16.68	16.68
<b>ND-PG</b>	1	0.2	432.29	428.12	429.51
<b>ND-PG</b>	1	0	11.12	12.51	12.51
<b>NR<sup>[a]</sup></b>	0	2	12,258.41	12,248.68	12,240.34
<b>NR<sup>[a]</sup></b>	0	0.2	1048.06	1045.28	1124.51
<b>NR blank<sup>[b]</sup></b>	0	n.d.	16.68	16.68	15.29
<b>Control (medium)</b>	0	0	13.90	15.29	15.29
<b>Control (PBS)</b>	0	0	19.46	22.24	20.85

[a] Nile Red was initially dissolved in DMSO at a concentration of  $10^{-4}$  M, and then diluted with medium. [b] Undiluted solution from the blank encapsulation experiment without the presence of nanocarrier.